5. Results and discussion

5.1. Introduction

Site characterisation requires knowledge of the vertical distribution of optical turbulence, the $C_N^2(h)$ profile. Such a profile may be obtained by turbulence and optical methods. Dr Igor Esau of NERSC has used LESNIC to compile a database of turbulence-resolving simulations named DATABASE64 (DB64). It consists of a collection of LESNIC runs for a stably stratified planetary boundary layer (SBL) over a homogeneous aerodynamically rough surface (Esau, 2004). The large-eddy simulation technique's ability to determine seeing conditions has been tested by employing the first eight runs from DB64. The $C_N^2(h)$ profiles and seeing parameter values obtained from DB64 results are presented and compared with observational results that have been published in the literature. Results from tests of the newly acquired seeing monitor hardware, and preliminary seeing measurements using the PSF technique, are also presented.

5.2. Turbulence method

5.2.1. Preliminary results using LESNIC

In Figure 5.1 and Table 5.1, respectively, profiles of the refractive index structure parameter $C_N^2(h)$ and the temperature structure parameter $C_T^2(h)$ as well as seeing parameter values for the first eight LESNIC runs from DB64, which cover a broad range of stability conditions in the PBL, as indicated in Section 3.2.3, are presented.

Profiles of C_N^2 and C_T^2 using DB64 Runs 1 to 8

Profiles of C_N^2 and C_T^2 for the first eight SBL runs of DB64, obtained as indicated in Section 3.2.3, are displayed in Figure 5.1.

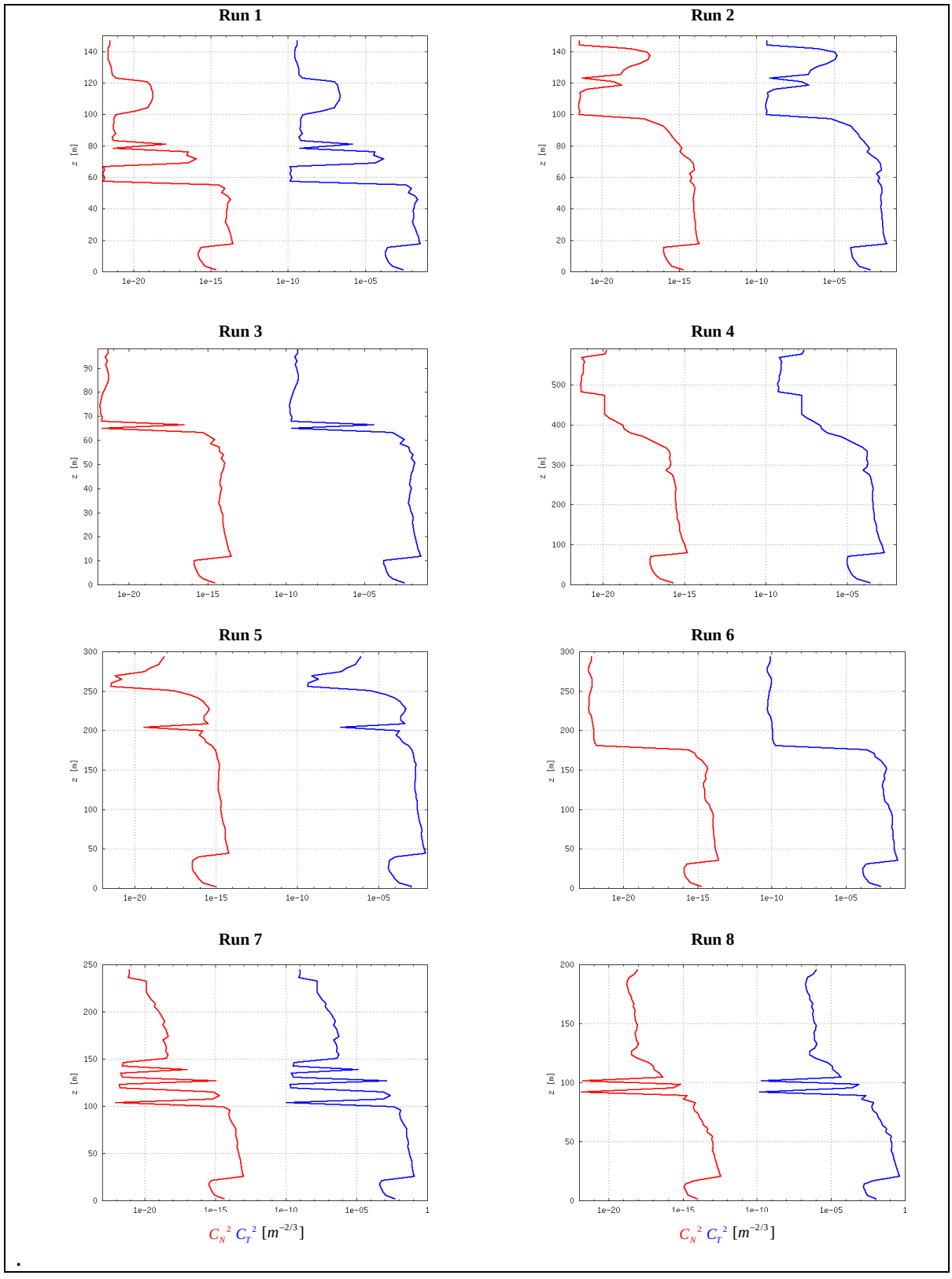

Figure 5.1. The simulated $C_N^2(h)$ and $C_T^2(h)$ log profiles for runs 1 to 8 of DB64

Seeing parameter values using DB64 Runs 1 to 8

Values of r_0 and ε_{FWHM} for the first eight SBL runs of DB64, obtained as indicated in Section 3.2.3 (with λ = 532 nm), are displayed in Table 5.1:

Table 5.1. Fried parameter value and seeing for the first eight runs in DB64.

Seeing parameters	**Run1**	**Run2**	**Run3**	**Run4**	**Run5**	**Run6**	**Run7**	**Run8**
r_0 (cm)	21	20	16	120	41	19	10	5
ε_{FWHM} (")	0.5	0.5	0.7	0.1	0.3	0.6	1.1	2.1

5.2.2. Results published in literature

Intense site testing campaigns have been taking place at Dome C in Antarctica, considered to be a site offering of the best astronomical seeing conditions on Earth. Balloon borne radiosonde measurements of C_N^2 profiles as well as seeing parameter values for Dome C have been made consistently over the past decade, and results are readily available in the literature. One such campaign, for which both C_N^2 profiles and seeing parameter values are available, is that which took place during the first winterover at Dome C in Antarctica in 2005 as reported on by Aristidi *et al*. (2009) and Trinquet *et al*. (2008).

The 2005 Dome C overwintering team launched meteorological balloon flights equipped with microthermal sensors to measure thermal fluctuations (mK) from Dome C to determine the vertical profile of the optical turbulence intensity $C_N^2(h)$ from the ground up to 20 km. The balloon transmitted the value of the refractive index structure constant every 1-2 seconds, which corresponds to a vertical resolution of 5-10 m. Meteorological parameters such as pressure, temperature, humidity and wind speed components were also provided by the soundings. Balloon launches started on the 15th of March 2005 (Flight Vol 520) during Autumn and concluded on the 19th of October (Flight Vol 575) during Spring.

Dome C is located at latitude 74.5° S on top of a local maximum of the Antarctic plateau, 3250 m above mean ice level. The Antarctic plateau is essentially free of topographic features. A surface roughness length of 0.005 m is allocated for such a featureless ice/snow surface. At the time of balloon launches, the AWS at Dome C provided surface measurements of wind speed, temperature, pressure and relative humidity (data and information obtained from IPEV/PNRA project "Routine Meteorological Observation at Station Concordia – www.climantartide.it"). Over the entire campaign, wind speeds ranged from 0-5 $m.s^{-1}$, temperatures from -74 °C to -52 °C (199-221 K), pressure from 618-658 mBar (61800-65800 Pa) and relative humidity from 14% to 60% (mostly either 14% or 15%).

Published results of observed $C_N^2(h)$ profiles

Thirty-two $C_N^2(h)$ profiles for the first 80 m above ground at Dome C in Antarctica (Aristidi *et al*. 2009) are displayed in Figure 5.2. The profiles are based on measurements made with balloon radio soundings, obtained during an astronomical site testing campaign at Dome C from 15 March (Flight Vol 520) – 19 October (Flight Vol 575) 2005 by Trinquet *et al*. (2008).

Published results of seeing parameter values

Seeing (ε_{FWHM}) for heights of 8 m and 33 m above the ice surface were retrieved from the above mentioned balloon profiles by Trinquet *et al*. (2008) by making use of Equation (2.21). Seeing at 8 m ranged from 0.5"-3.6" while that at 33 m ranged from 0.2"-2.5" over the entire campaign. These seeing values correspond to Fried parameter (r_0) values of 22 cm to 3 cm at 8 m and 54 cm to 4 cm at 33 m (for λ = 532 nm).

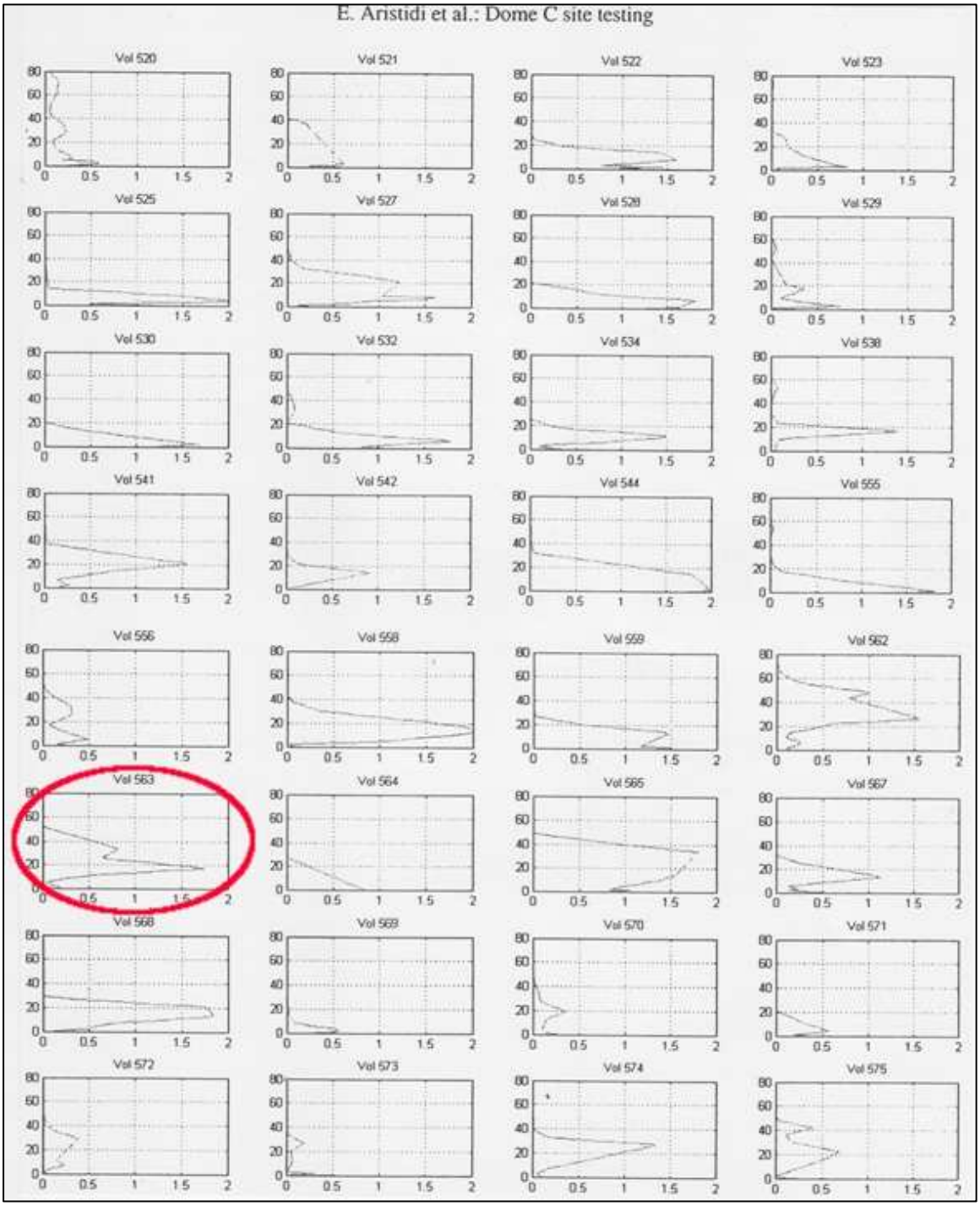

Figure 5.2. The observed $C_N^2(h)$ profiles obtained during site testing at Dome C in Antarctica (source: Aristidi *et al*., 2009). The value of $C_N^2(h)$ is indicated on a linear scale on the horizontal axis in units of $[10^{-13}\ m^{-2/3}]$ while the height above ground is displayed in [m] on the vertical axis. Flight Vol 563, circled in red, was utilized for comparison purposes.

5.2.3. Comparison of simulated and published results

Simulated vertical profiles of $C_N^2(h)$ and seeing parameter values have been obtained by making use of DB64 results for the nocturnal boundary layer. These profiles and values have been compared with observational profiles and seeing parameter values from literature. Such a comparison is necessary to verify that the profiles produced by turbulence modelling are at least similar in nature and order of magnitude to measured $C_N^2(h)$ profiles, and that seeing parameter values are of a similar order of magnitude to values appearing in the literature. This will then provide either negative or positive assurance that LESNIC gives reasonable results when its *a-priori* parameters are similar to some extent to the experimentally derived results.

Simulated results for $C_N^2(h)$ profiles with linear scale on x-axis

Profiles of $C_N^2(h)$ from DB64 were plotted on a logarithmic scale for the C_N^2-axis. Observational profiles of $C_N^2(h)$ from literature are displayed on a linear scale. Profiles of $C_N^2(h)$ for the eight runs of DB64, re-plotted on a linear scale for comparison purposes, as well as the LESNIC external control parameters for each run, are displayed in Figure 5.3.

Comparison of $C_N^2(h)$ profiles

Profiles of $C_N^2(h)$ obtained from the first 8 runs of DB64 by turbulence-modelling of the nocturnal boundary layer with LESNIC (Figure 5.3) were compared with 32 observational profiles (Figure 5.2) measured by balloon radio sounding at Dome C in Antarctica during the austral winter of 2005 by the Dome C overwintering team as part of an astronomical site testing campaign as reported in the literature (Aristidi *et al*. 2009).

Such a comparison is possible for the following reason: The study of turbulence in the PBL is based on the solution of the Reynolds-averaged Navier-Stokes equations, which present the conservation laws of momentum, energy and fluxes. The particular realisation of turbulence characteristics is calculated subject to boundary conditions at the top and bottom of the PBL. It is then possible to compare the numerical results with experimental data which have been collected at the same boundary conditions. Generally, the turbulence

Run 1

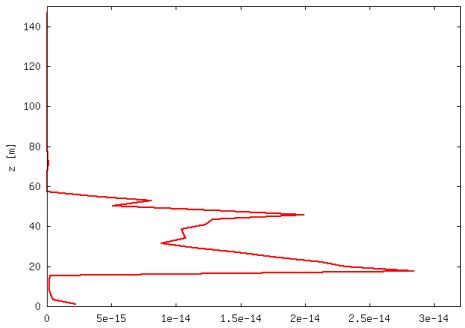

External control parameters

Domain size [m]	**300x300x150**
Latitude [°]	**70**
Surface roughness [m]	**0.05**
Surface heat flux [K.m.s^{-1}]	**-0.002**
Geostrophic wind [m.s^{-1}]	**3**
Surface temperature [K]	**283**
Surface pressure [Pa]	**90500**
Relative humidity [%]	**70**

Run 2

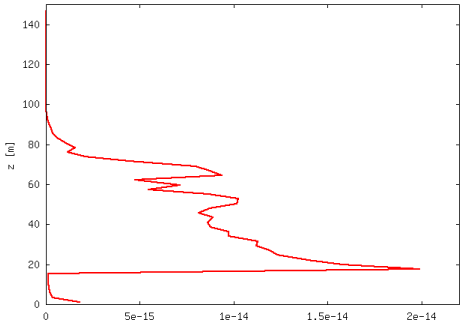

External control parameters

Domain size [m]	**200x200x150**
Latitude [°]	**70**
Surface roughness [m]	**0.07**
Surface heat flux [K.m.s^{-1}]	**-0.002**
Geostrophic wind [m.s^{-1}]	**3**
Surface temperature [K]	**283**
Surface pressure [Pa]	**90500**
Relative humidity [%]	**70**

Run 3

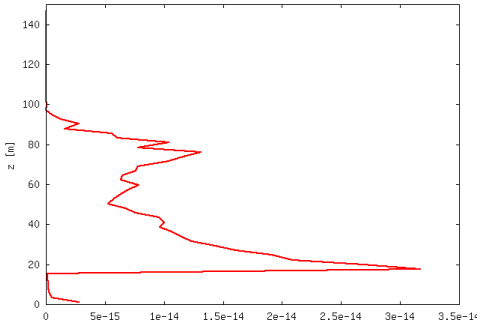

External control parameters

Domain size [m]	**150x150x100**
Latitude [°]	**90**
Surface roughness [m]	**0.03**
Surface heat flux [K.m.s^{-1}]	**-0.002**
Geostrophic wind [m.s^{-1}]	**3**
Surface temperature [K]	**283**
Surface pressure [Pa]	**90500**
Relative humidity [%]	**70**

Run 4

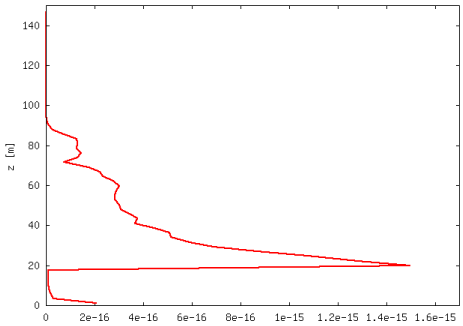

$C_N^2\ [m^{-2/3}]$

External control parameters

Not available

Figure 5.3. The $C_N^2(h)$ linear profile and LESNIC external control parameters for runs 1 to 8.

Run 5

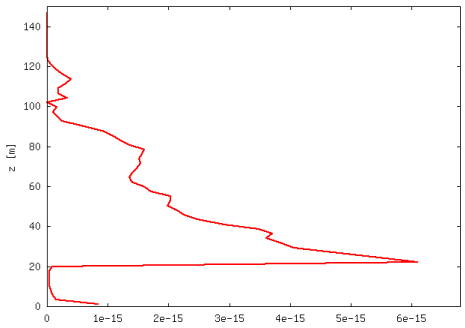

External control parameters

Domain size [m]	**450x450x300**
Latitude [°]	**45**
Surface roughness [m]	**0.1**
Surface heat flux [K.m.s^{-1}]	**-0.003**
Geostrophic wind [m.s^{-1}]	**5**
Surface temperature [K]	**283**
Surface pressure [Pa]	**90500**
Relative humidity [%]	**70**

Run 6

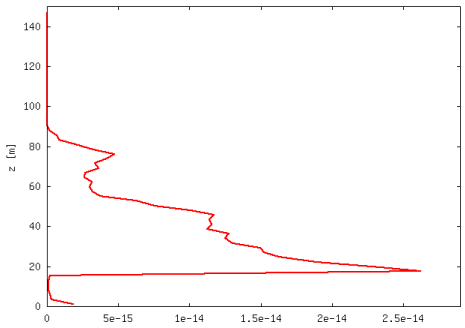

External control parameters

Domain size [m]	**400x400x300**
Latitude [°]	**45**
Surface roughness [m]	**0.1**
Surface heat flux [K.m.s^{-1}]	**-0.004**
Geostrophic wind [m.s^{-1}]	**5**
Surface temperature [K]	**283**
Surface pressure [Pa]	**90500**
Relative humidity [%]	**70**

Run 7

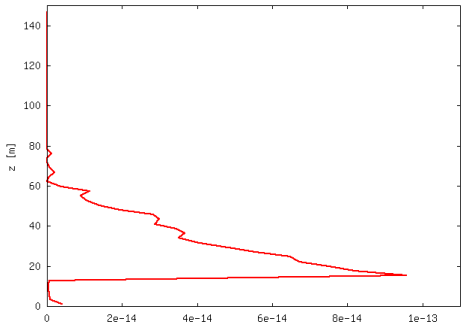

External control parameters

Domain size [m]	**350x350x250**
Latitude [°]	**45**
Surface roughness [m]	**0.1**
Surface heat flux [K.m.s^{-1}]	**-0.005**
Geostrophic wind [m.s^{-1}]	**5**
Surface temperature [K]	**283**
Surface pressure [Pa]	**90500**
Relative humidity [%]	**70**

Run 8

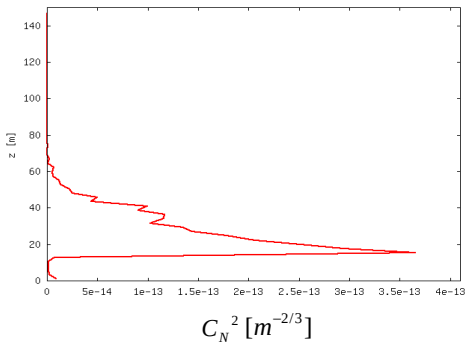

External control parameters

Domain size [m]	**300x300x200**
Latitude [°]	**45**
Surface roughness [m]	**0.1**
Surface heat flux [K.m.s^{-1}]	**-0.006**
Geostrophic wind [m.s^{-1}]	**5**
Surface temperature [K]	**283**
Surface pressure [Pa]	**90500**
Relative humidity [%]	**70**

Figure 5.3 (continued from the previous page). The $C_N^2(h)$ linear profile and LESNIC external control parameters for runs 1 to 8.

is determined by the geostrophic wind and the temperature difference between the top and bottom of the PBL ($\Delta T > 0$ corresponds to stable stratification, which is relevant to astronomical seeing conditions). Therefore PBL turbulence will be the same for hot climatic conditions (for example, $\Delta T = T_{top} - T_{bottom} = 35°C - 30°C = 5°C$) as it is for very cold climatic conditions, such as those of Antarctica (for example, $\Delta T = T_{top} - T_{bottom} = -30°C - (-35°C) = 5°C$).

LESNIC can only be used to provide a generalised profile based on the input parameters as indicated in Figure 5.3. These control parameters do not necessarily correspond with those prevalent at Dome C (meteorological surface conditions for Dome C are discussed in Section 5.2.2), and a direct comparison is therefore not possible. However, by comparing the profiles, it is possible to determine whether the profiles produced by LESNIC are at least of roughly the same shape and scale as the observed profiles, and whether LESNIC can therefore be used as a general tool to evaluate sites at some level.

In comparing the simulated $C_N^2(h)$ profiles of Figure 5.3 with the observed profiles of Figure 5.2, it is immediately apparent that the simulated profiles, in general, do not appear similar in shape to the observed profiles. However, from Figure 5.3, it is also apparent that the observed profiles are themselves dissimilar in shape for the entire observation period. Profiles change with every flight. Some profiles include a second peak, while others do not. The eight simulated profiles are similar in shape and also do resemble a few of the observational profiles in shape, especially Flights Vol 562 and 563 and, to a lesser extent, Flights Vol 538, 541 and 574.

One of the observed profiles which compares favourably in shape with the simulated profiles, Flight Vol 563, is displayed in Figure 5.4. The simulated profile produced in Run 8 is displayed in Figure 5.5 for comparison. The two $C_N^2(h)$ profiles compare well for similarity in shape and order-of-magnitude.

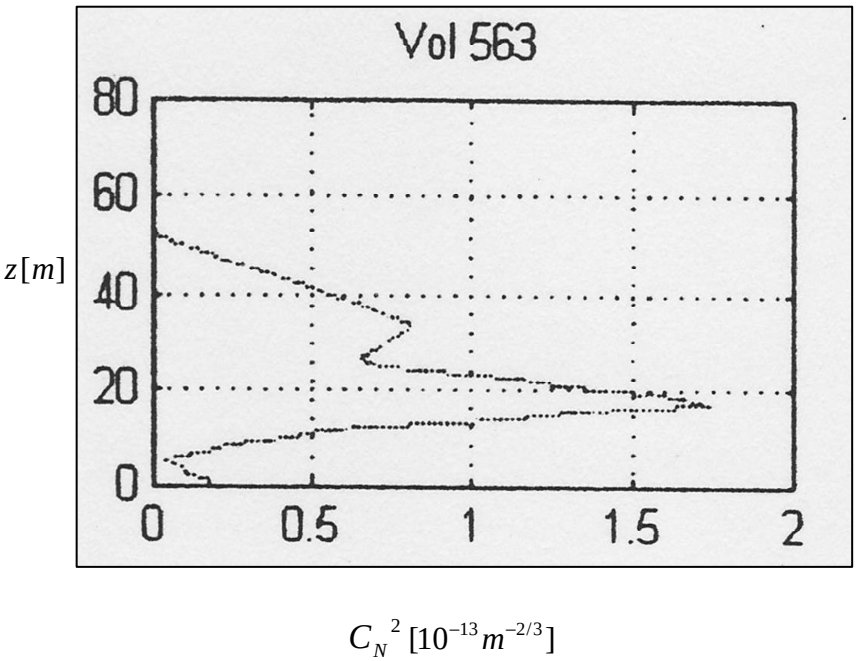

Figure 5.4. Flight Vol 563 $C_N^2(h)$ profile measured at Dome C, Antarctica (source: Aristidi *et al*., 2009).

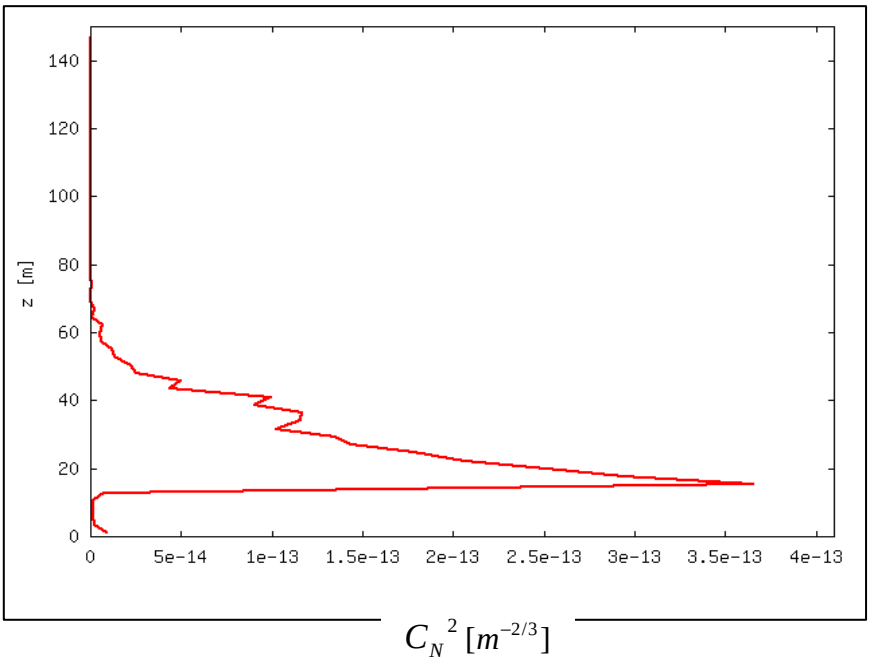

Figure 5.5. The LESNIC-modelled $C_N^2(h)$ profile for run 8 from DB64.

With regards to scale, for the observed profiles, Trinquet *et al*. (2008) reports C_N^2 values of $3\text{x}10^{-14}$ $m^{-2/3}$ near the ground, which rapidly decreases to 10^{-17} $m^{-2/3}$ at a height of 100 m. Simulated profiles display C_N^2 values in the region of 10^{-16}-10^{-13} $m^{-2/3}$. The quantitative

shapes of the simulated profiles, when compared to the observational profiles from literature, are generally quite reasonable.

Comparison of r_0 and ε_{FWHM}

Seeing parameter values calculated from the simulated profiles range from 0.1" to 2.1" for ε_{FWHM} and from 120 cm to 5 cm for r_0. Seeing parameter values retrieved from observed profiles range from 0.5" to 3.6" for ε_{FWHM} and from 22 cm to 3 cm for r_0 at 8 m and from 0.2" to 2.5" for ε_{FWHM} and from 54 cm to 4 cm for r_0 at 33 m. Seeing parameter values obtained from the model are therefore in close agreement with observed values (from literature).

5.3. Optical method

A recent trip to Matjiesfontein presented an opportunity to test newly acquired seeing monitor equipment. Preliminary seeing measurements for the PSF seeing experiment were performed as follows:

The seeing monitor setup consisted of the Meade 14" f/10 SCT with GOTO fork-arm mount supported by the heavy-duty tripod as well as the 4.4-µm Point Grey Grasshopper GRAS-20S4M monochrome CCD camera attached to a flip mirror on the exit pupil of the telescope. The seeing monitor was deployed outside the Matjiesfontein courthouse. Dark, clear, dry and windless conditions prevailed. Considerable ambient light was present. The two visible components of the Alpha Centauri binary system, Alpha Centauri A and B (α Cen AB) were centred in an eye piece which was also attached to the flip mirror. The CCD camera was set to capture short exposure images of ~ 1 ms at a frame rate of ~ 7 fps.

For the combination of:

- the 14" (= 350 mm) aperture diameter telescope with a focal ratio of f/10, therefore focal length of 3500 mm as given by Equation (4.1), and
- a CCD camera with 4.4-µm pixel size,

the image scale is given by Equation (3.5) as being 0.26 arc-second per pixel.

5.3.1. Point Spread Function (PSF) seeing experiment: calibration results using αCen binary separation

The first test entailed seeing monitor setup verification, i.e. determining whether the seeing monitor setup would perform as expected. The short 1-ms exposure images of the Alpha Centauri AB binary system captured at a frame rate of ~ 7 fps were analysed to determine the binary separation given by the seeing monitor setup. This observed separation could then be compared with the known separation according to the literature.

Image analysis thus consisted of the following –

1. Finding the separation between the principle, αCenA, and the companion, αCenB, of the Alpha Centauri AB binary star system:

   Image uploaded into GIMP image editor to provide x and y coordinates of pixels using Treshold tool to locate pixel with peak intensity value at centre of star image for both stars.

   Separation of components in CCD camera pixels is given by

   $$d = \sqrt{(\Delta x)^2 + (\Delta y)^2}. \tag{5.1}$$

   Separation of components in arc-seconds is given by

   $$\rho = 0.26''/\text{pixel} \times d \text{ pixels}. \tag{5.2}$$

   From Table 5.2, for the 10 images observed and captured with the seeing monitor setup, the average separation of the binary star components was calculated to be 5.3" ± 0.3".
2. Comparing the observed value for the binary star separation of 5.3" to the separation given by the literature of 5.4" (from The Sixth Catalog of Orbits of Visual Binary Stars, 2006).

The close agreement between the observed and stated values verifies and validates the operation of the current seeing monitor setup for the PSF seeing experiment.

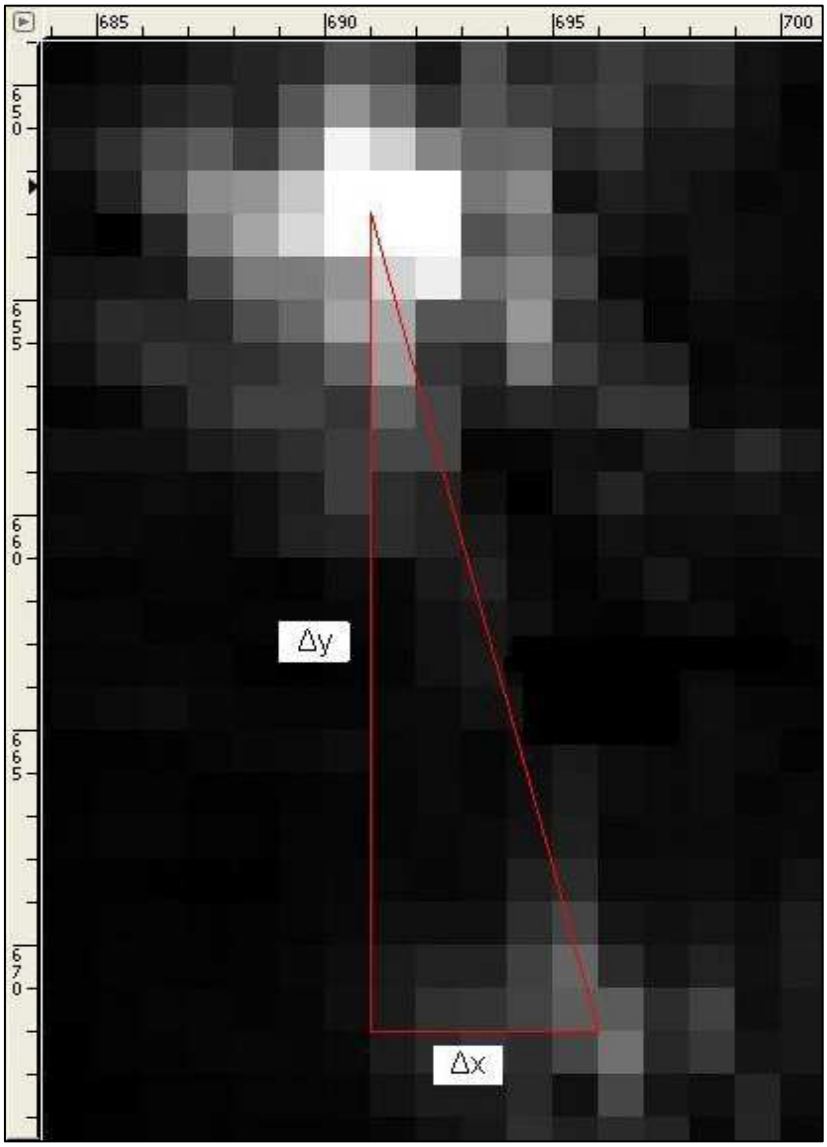

Figure 5.6. Separation of binary stars were found by importing captured images into an image editor, locating the pixel with peak intensity at the centres of both stars and calculating their separation.

Table 5.2. PSF seeing experiment: verification of seeing monitor setup by observing binary star separation.
Image no. 2 was a non-observation – the companion, αCenB, was not observed, probably being obscured by high thin cloud.

Image scale = 0.26"/pixel	**αCenA**		**αCenB**							
Image	**x**	**y**	**x**	**y**	$x_{\alpha 2}-x_{\alpha 1}$	$y_{\alpha 2}-y_{\alpha 1}$	$(x_{\alpha 2}-x_{\alpha 1})^2$	$(y_{\alpha 2}-y_{\alpha 1})^2$	**d**	**ρ**
no.	**pixels**	**pixels**	**pixels**	**pixels**	**pixels**	**pixels**	**pixels**	**pixels**	**pixels**	**"**
0	691	653	696	672	5	19	25	361	19.65	5.1
1	692	654	696	673	4	19	16	361	19.42	5.0
2	691	657	-	-	-	-	-	-	-	
3	689	653	694	675	5	22	25	484	22.56	5.9
4	693	654	696	673	3	19	9	361	19.24	5.0
5	691	655	695	675	4	20	16	400	20.40	5.3
6	689	655	696	676	7	21	49	441	22.14	5.8
7	688	655	694	674	6	19	36	361	19.92	5.2
8	691	653	695	672	4	19	16	361	19.42	5.0
9	688	655	693	675	5	20	25	400	20.62	5.4
Average separation (")									**20.37**	**5.3**
+/-									1.21	0.3
Separation from literature (") (2012)										**5.4**

5.3.2. Point Spread Function (PSF) seeing experiment: initial results with αCenA

The second test entailed performing a preliminary PSF seeing experiment. Images of the brightest star of the binary system, αCenA, which had been captured outside the Matjiesfontein courthouse, were analysed to determine the FWHM of the star's intensity profile and thus the seeing.

Image analysis thus consisted of the following –

1. Obtaining four intensity profiles of αCenA for each of the 10 images:

   Image uploaded into AstroArt astronomical image processing program and pixel lines drawn through centre of star image (as determined in previous experiment), providing the four intensity profiles for each image.

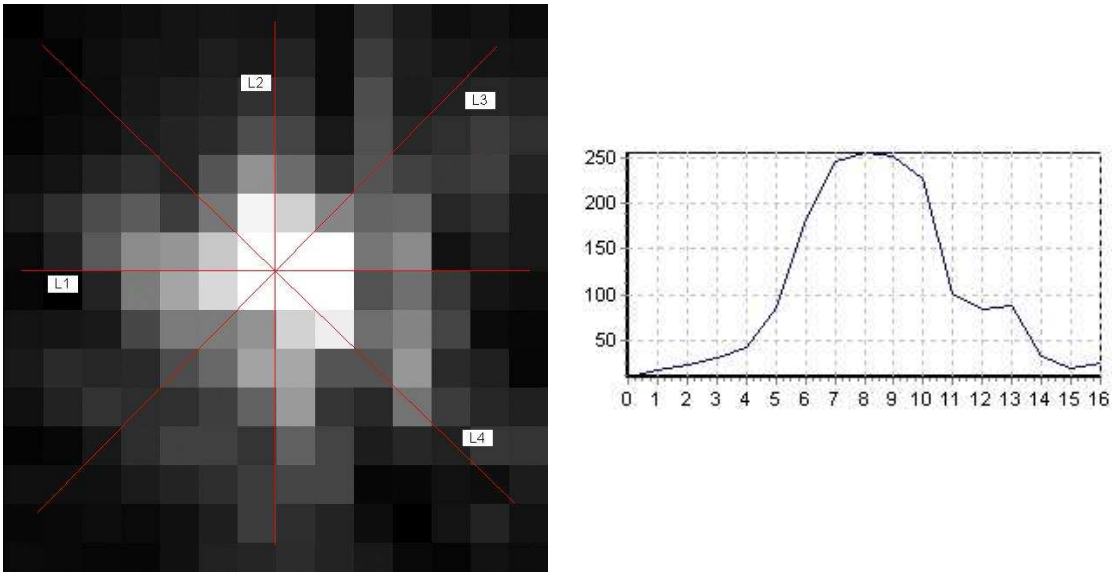

Figure 5.7. Intensity profiles were obtained by importing captured images into an astro-imaging application and analysing the images.

2. Performing a nonlinear regression analysis with a Gaussian fit to the star's intensity profile (4 profiles per image, 10 images):

   F`orm of Gaussian equation is given by

$$y = ae^{\left[-0.5\left(\frac{x-x_0}{b}\right)^2\right]}. \qquad (5.3)$$

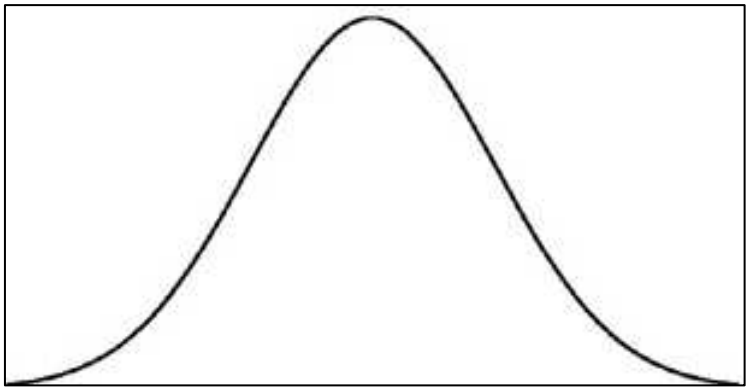

Figure 5.8. Bell-shaped Gaussian distribution curve.

3. Obtaining the standard deviation (b in pixels, see Table 5.3), from the Gaussian distribution, of the FWHM of the star's intensity profile.
4. Obtaining the standard deviation σ (Table 5.3) in arc-seconds (by converting from pixels to arc-seconds using the image scale)

$$\sigma\,[''] = 0.26''/\,\text{pixel} \times \sigma\,[\text{pixels}]. \tag{5.4}$$

5. Obtaining the FWHM, and thus the seeing ε_{FWHM} (Table 5.3), from the standard deviation σ according to Equation (3.7a)

$$\varepsilon_{FWHM} = FWHM = 2.355 \times \sigma. \tag{5.5}$$

The average seeing measured outside the Matjiesfontein courthouse was $2.1'' \pm 0.47''$, which is very good seeing conditions given the surroundings. It also compares well with previous seeing measurements at Matjiesfontein which delivered seeing of 1-2" (Combrinck *et al.*, 2007).

Table 5.3. PSF seeing experiment: initial seeing results at Matjiesfontein with αCenA.

Image scale = 0.26"/pixel
σ (") = 0.26* b
ε_{FWHM} (") = FWHM (") = 2.355*σ

Image no.

	0			**1**			**2**			**3**			**4**		
	b	**σ**	ε_{FWHM}	**b**	**σ**	ε_{FWHM}	**b**	**σ**	ε_{FWHM}	**b**	**σ**	ε_{FWHM}	**b**	**σ**	ε_{FWHM}
Pixel line	**pixels**	**"**	**"**	**pixels**	**"**	**"**	**pixels**	**"**	**"**	**pixels**	**"**	**"**	**pixels**	**"**	**"**
1	2.424	0.63	**1.5**	2.946	0.77	**1.8**	3.947	1.03	**2.4**	2.095	0.54	**1.3**	5.512	1.43	**3.4**
2	2.647	0.69	**1.6**	2.660	0.69	**1.6**	5.722	1.49	**3.5**	2.891	0.75	**1.8**	3.853	1.00	**2.4**
3	2.133	0.55	**1.3**	2.632	0.68	**1.6**	3.957	1.03	**2.4**	2.720	0.71	**1.7**	3.465	0.90	**2.1**
4	2.525	0.66	**1.5**	3.182	0.83	**1.9**	3.942	1.02	**2.4**	4.178	1.09	**2.6**	5.165	1.34	**3.2**
Average/image (")			**1.5**			**1.7**			**2.7**			**1.8**			**2.8**

Image no.

	5			**6**			**7**			**8**			**9**		
	b	**σ**	ε_{FWHM}	**b**	**σ**	ε_{FWHM}	**b**	**σ**	ε_{FWHM}	**b**	**σ**	ε_{FWHM}	**b**	**σ**	ε_{FWHM}
Pixel line	**pixels**	**"**	**"**	**pixels**	**"**	**"**	**pixels**	**"**	**"**	**pixels**	**"**	**"**	**pixels**	**"**	**"**
1	2.896	0.75	**1.8**	6.541	1.70	**4.0**	2.774	0.72	**1.7**	3.496	0.91	**2.1**	3.008	0.78	**1.8**
2	2.375	0.62	**1.5**	4.712	1.23	**2.9**	2.527	0.66	**1.5**	4.158	1.08	**2.5**	3.166	0.82	**1.9**
3	3.939	1.02	**2.4**	3.382	0.88	**2.1**	2.656	0.69	**1.6**	2.825	0.73	**1.7**	3.248	0.84	**2.0**
4	3.980	1.03	**2.4**	3.972	1.03	**2.4**	3.179	0.83	**1.9**	2.504	0.65	**1.5**	3.467	0.90	**2.1**
Average/image (")			**2.0**			**2.8**			**1.7**			**2.0**			**2.0**

Overall average (")	**2.1**	+/-	0.5